



저작자표시-비영리-변경금지 2.0 대한민국

이용자는 아래의 조건을 따르는 경우에 한하여 자유롭게

- 이 저작물을 복제, 배포, 전송, 전시, 공연 및 방송할 수 있습니다.

다음과 같은 조건을 따라야 합니다:



저작자표시. 귀하는 원저작자를 표시하여야 합니다.



비영리. 귀하는 이 저작물을 영리 목적으로 이용할 수 없습니다.



변경금지. 귀하는 이 저작물을 개작, 변형 또는 가공할 수 없습니다.

- 귀하는, 이 저작물의 재이용이나 배포의 경우, 이 저작물에 적용된 이용허락조건을 명확하게 나타내어야 합니다.
- 저작권자로부터 별도의 허가를 받으면 이러한 조건들은 적용되지 않습니다.

저작권법에 따른 이용자의 권리는 위의 내용에 의하여 영향을 받지 않습니다.

이것은 [이용허락규약\(Legal Code\)](#)을 이해하기 쉽게 요약한 것입니다.

[Disclaimer](#)

# Hypoxia measurement of gastric conduit after esophagectomy and gastric reconstruction in rats



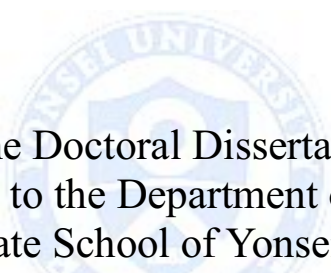
Seong Yong Park

Department of Medicine

The Graduate School, Yonsei University

# Hypoxia measurement of gastric conduit after esophagectomy and gastric reconstruction in rats

Directed by Professor Kyung Young Chung



The Doctoral Dissertation  
submitted to the Department of Medicine,  
the Graduate School of Yonsei University  
in partial fulfillment of the requirements for the degree  
of Doctor of Philosophy

Seong Yong Park

June 2015

This certifies that the Doctoral  
Dissertation of Seong Yong Park is  
approved.

-----  
Thesis Supervisor: Kyung Yong Chung

-----  
Thesis Committee Member: Won Joon Kang

-----  
Thesis Committee Member: Chang Hyun Kang

-----  
Thesis Committee Member: Chul Ho Kim

-----  
Thesis Committee Member: Ki Taek Nam

The Graduate School  
Yonsei University

June 2015

## ACKNOWLEDGEMENTS

First of all, I would like to show my respect and thank Professor Kyung Young Chung, not only for directing me as a student but also giving me opportunities to be a better thoracic surgeon. I would also like to thank Professor Won Jun Kang for teaching me how to actually research, perform the experiments and write a thesis. They are the mentors I sincerely respect. I would like to express my sincere gratitude to Professor Chang Hyun Kang, Chul Ho Kim and Ki Taek Nam for their review and comments. I also appreciate Professor Arthor Cho, Ju Ri Chae and Ye Lim Cho for their advising and helping the experiments.

I thank my parents and parents-in-law for supporting me all the time. I would like to thank my wife, Sae Jung Cha for being next to me all the time. I would like to mention my two sons and I would like to say I love you all.

Seong Yong Park

## <TABLE OF CONTENTS>

ABSTRACT .....	1
I. INTRODUCTION .....	3
II. MATERIALS AND METHODS .....	6
1. Operation .....	6
2. Fluorescence imaging .....	8
3. MicroPET scan .....	8
4. Autoradiography .....	9
5. Histologic evaluation and immunohistochemistry .....	9
6. Statistical analysis .....	10
III. RESULTS .....	11
1. Establishment of rat esophagectomy animal model .....	11
2. Fluorescent imaging .....	12
3. MicroPET scan .....	14
4. Autoradiography .....	16
5. Immunohistochemistry .....	17
IV. DISCUSSION .....	20
V. CONCLUSION .....	26
REFERENCES .....	27
ABSTRACT (IN KOREAN) .....	30

## LIST OF FIGURES

Figure 1. Operative view .....	7
Figure 2. Rat esophagectomy animal model .....	11
Figure 3. Fluorescent imaging .....	13
Figure 4. MicorPET imaging .....	15
Figure 5. Autoradiography .....	16
Figure 6. Immunohistochemistry .....	18
Figure 7. The correlations between expression of immunohistochemistry and PET parameters .....	19

## **ABSTRACT**

Hypoxia measurement of gastric conduit after esophagectomy and gastric reconstruction in rats

Seong Yong Park

*Department of Medicine*

*The Graduate School, Yonsei University*

(Directed by Professor Kyung Young Chung)

Conduit ischemia is an important phenomenon related to anastomosis leakage and stricture after esophagectomy and gastric reconstruction. Clinical detection and measurement of ischemia of the gastric conduit during the postoperative period is important but difficult. In this study, optical fluorescence imaging and hypoxia Positron emission tomography (PET) imaging was studied whether it could detect the ischemia of gastric conduit in rat esophagectomy model. A rat esophagectomy model was created using 12-16-week-old, 300-350 g male Sprague-Dawley rats. In the operation group partial gastric devascularization was performed by ligating the left gastric artery and the short gastric arteries and an esophagogastric anastomosis was performed. In the control group, the esophageal-gastric junction was incised and suturing was performed without

gastric devascularization. Optical fluorescence imaging with hypoxia agent and PET images with  $^{64}\text{Cu}$ -diacetyl-bis (N4-methylsemicarbazone) ( $^{64}\text{Cu}$ -ATSM) were taken 24 h after the initial operation. In animal experiment, optical fluorescence imaging with hypoxia agent could not detect conduit ischemia. Hypoxia imaging with hypoxia tracer  $^{64}\text{Cu}$ -ATSM revealed  $^{64}\text{Cu}$ -ATSM uptake at the fundus in the operation group 3 h after  $^{64}\text{Cu}$ -ATSM injection. The maximum percentage of the injected dose per gram of tissue was higher in the operation group ( $0.047 \pm 0.015$  vs.  $0.026 \pm 0.006$ ,  $p=0.021$ ). The fundus/liver ratio was also higher in the operation group ( $0.541 \pm 0.126$  vs.  $0.278 \pm 0.049$ ,  $p=0.002$ ). Upon autoradiography,  $^{64}\text{Cu}$ -ATSM uptake was observed in the fundus in the operation group, and was well-correlated to that observed on the PET image. Upon immunohistochemistry, expressions of hypoxia-inducible factor 1 $\alpha$  and pimonidazole were significantly increased at the fundus and lesser curvature compared to the greater curvature in the operation group. In conclusion, hypoxia PET imaging with  $^{64}\text{Cu}$ -ATSM can detect ischemia in a rat esophagectomy model. Further clinical studies are needed to verify whether hypoxia imaging may be useful in humans.

---

**Key words:** esophagectomy, conduit ischemia, hypoxia imaging, PET

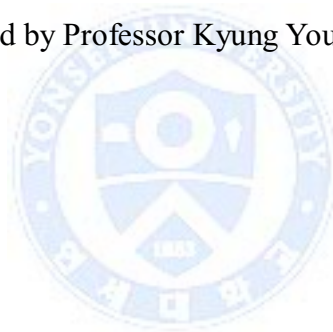
Hypoxia measurement of gastric conduit after esophagectomy and gastric  
reconstruction in rats

Seong Yong Park

*Department of Medicine*

*The Graduate School, Yonsei University*

(Directed by Professor Kyung Young Chung)



## **I. INTRODUCTION**

Esophagectomy is the treatment of choice for early and locally advanced esophageal cancer. Esophageal reconstruction is usually performed via gastric pull-up and esophagogastrostomy<sup>1</sup>; however, leakage through an esophagogastric anastomosis complicates 5-20% of all esophagectomies.<sup>1,2</sup> Esophagectomy for esophageal cancer is associated with an operative mortality of approximately 10%,<sup>1</sup> and between 30% and 50% of these deaths are associated with anastomotic leakage.<sup>3</sup> Therefore, elimination of anastomotic leaks would greatly reduce the morbidity and mortality associated with esophagectomy.<sup>2</sup> Several factors are linked to anastomosis leakage; ischemia of

the gastric conduit is a major factor. Additionally, clinical detection and measurement of ischemia of the gastric conduit during the postoperative period is difficult. Oezcelik et al. recently reported that chest computed tomography (CT) was not useful for detecting conduit ischemia or anastomosis breakdown, and that endoscopy was more valuable than chest CT for detecting ischemia.<sup>4</sup> However, endoscopy is invasive and can damage anastomoses; moreover, grading of gastric mucosal ischemia by an endoscopist can be subjective. Therefore, imaging modality for detecting the conduit ischemia is needed in clinical situations.

Recently, several kinds of imaging modalities have been studied for detecting the hypoxia and ischemia. Among those, two types of available imaging modalities could be considered for conduit ischemia of gastric conduit could. First, optical imaging that uses nonionizing radiation in the visible to near infrared wave lengths could be applied. Optical imaging has been applied in many clinical situations, like autofluorescence imaging which detects ocular lesion or gastrointestinal malignancies such early esophageal squamous cell carcinoma, and organic fluorophores imaging which detects metastatic lymph nodes in breast cancer. By using exogenous fluorophores which reacts with low oxygen level, the fluorescent optical imaging might detect the hypoxia area in gastric conduit.

Second, nuclear imaging techniques, particularly positron emission tomography (PET), are best when used to detect and assess tissue hypoxia

because of the availability of several radiotracers that are selectively entrapped within regions of hypoxic tissue.<sup>5</sup> Hypoxia PET imaging has been applied to cerebral stroke and cancer imaging. We hypothesized that hypoxia PET imaging would detect ischemic areas of the gastric conduit after esophagectomy and esophagogastrostomy, because ischemia would be indicated by hypoxia of a particular tissue or organ.

This experimental animal study was conducted to verify whether two imaging modalities, optical fluorescent imaging and hypoxia PET imaging could detect ischemia of a gastric conduit or not by using the rat esophagectomy model.



## II. MATERIALS AND METHODS

### 1. Operation

The current study was approved by the institutional Animal Care and Use Committee (No. 2013-0350) of Yonsei University, College of Medicine. Based on previous studies, a rat esophagectomy model was created using 12-16-week old, 300-350-g, male Sprague-Dawley rats.<sup>5,6</sup> Twelve rats were housed (3 per cage) in conventional suspension cages, and given food and water ad libitum until the time of surgery. A 3-cm median laparotomy incision was made under inhaled sevoflurane anesthesia using a rodent ventilator. In the operation group, partial gastric devascularization was performed by ligating the left gastric artery and the short gastric arteries (Fig 1A and 1B). The esophageal-gastric junction was then incised around 50% of the circumference. This left a small bridge of tissue at posterior part of esophagogastric junction for simplifying the anastomotic suturing. The esophagogastric anastomosis was sutured with interrupted 5-0 polypropylene sutures (Fig. 1C, 1D and 1E). All laparotomy incisions were closed with continuous 3-0 silk sutures. Animals were allowed free access to water only after operation. The control group underwent only incision of the esophageal-gastric junction; suturing was performed without partial gastric devascularization.

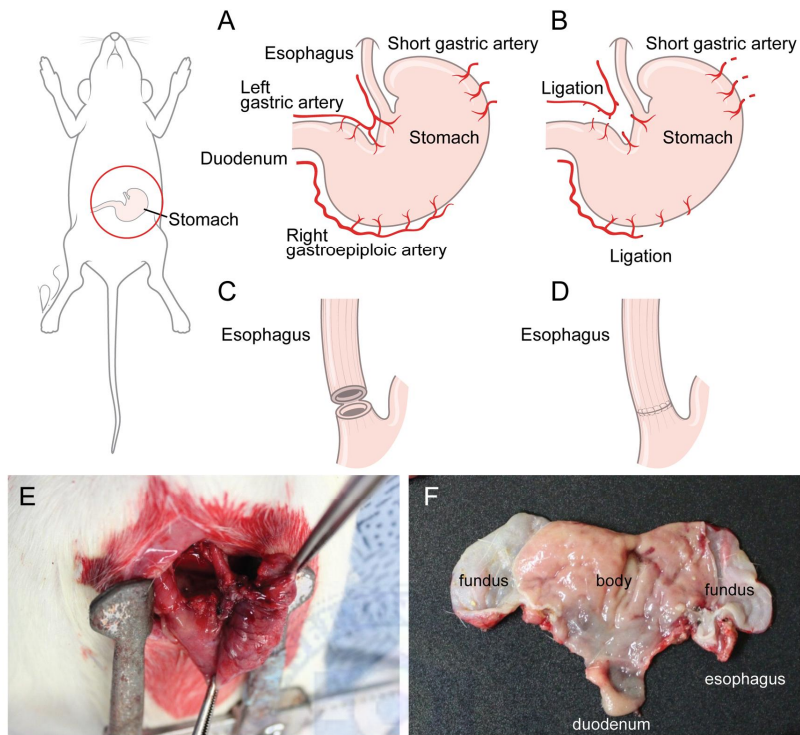


**Figure 1.** Operative view. A. Normal vascular anatomy of rat. B. Partial devascularization was done by ligating the left gastric artery and short gastric arteries. C. The esophageal-gastric junction was then incised around 50% of the circumference. D. The esophagogastric anastomosis was sutured with interrupted 5-0 polypropylene sutures. E. Operative pictures after all procedures in operation group. F. After microPET imaging, the stomach was incised along the lesser curvature to obtain autoradiographic images.

## 2. Fluorescence imaging

Fluorescence imaging was performed using IVIS fluorescent camera (IVIS® Spectrum in vivo imaging system, Perkin Elmer). Hypoxia fluorescent probe HypoxiSense 680 (PerkinElmer) was which is quenched by oxygen and is increased in response to low levels of oxygen was used. After 2 nmol (100 µL) of HypoxiSense 680 was injected via tail-vein, fluorescent imaging was taken for extracted whole stomach at 680nm, for 5 seconds of exposures, 6 hours after injection. Fluorescent imaging was taken in control and operation group together, for unifying the exposure time. A region of interest (ROI) was drawn at whole stomach and optical signals were quantified and compared.

## 3. MicroPET scan

PET imaging was performed using a microPET rodent scanner (Siemens Inveon MicroPET) 24 h after the initial operation. Before PET imaging, water and food were permitted for 12 h. After fasting, the animals were injected with 200 µCi  $^{64}\text{Cu}$ -diacetyl-bis (N4-methylsemicarbazone) ( $^{64}\text{Cu}$ -ATSM) via the tail vein and 120 mg/kg pimonidazole intraperitoneally. Each rat was placed near the center of the field of view of the microPET 3 h after  $^{64}\text{Cu}$ -ATSM injection, where the highest image resolution and sensitivity were available. Static imaging was performed for 20 min at 3 h after injection of ATSM. A region of interest (ROI) was drawn in the gastric fundus and a dose of  $^{64}\text{Cu}$ -ATSM semiquantitated to the “max percent” value was injected per gram of

tissue (%ID/g). The fundus/liver ratio was calculated by dividing the %ID/g of the fundus by the %ID/g of the liver. A reference region of the liver was drawn in the right hepatic lobe. Image analysis was done by professional program, PMOD (version 3.6003A).

#### **4. Autoradiography**

Immediately after microPET imaging, the rats were euthanized and the stomachs excised along the lesser curvature (Figure 1F). Excised stomachs were transferred to a chilled autoradiography cassette and stored for 12 h at -4°C. Screens were read using an FLA7000 scanner (Fujifilm, Tokyo, Japan). ROIs were selected on the greater curvature of the stomach where the blood supply was intact, and in the fundus where the blood supply was not intact because of partial devascularization of the stomach. The optical densities of autoradiographic signals were measured using Multi Gauge 3.2 software (Fujifilm, Tokyo, Japan). Autoradiographic images and ROIs were compared between the two groups.

#### **5. Histological evaluation and immunohistochemistry**

After autoradiography, stomach tissue was fixed in 2% (v/v) formalin, embedded in paraffin for 24 h, sectioned at 5- m thickness, and stained with hematoxylin and eosin (H&E). Four sections were prepared from each rat; two from the great curvature of the stomach (where the blood supply was intact) and

two from the fundus where the blood supply was not intact because of partial devascularization of the stomach. These sections were from the same ROIs evaluated via autoradiography. From the 12 rats, a total of 48 sections was prepared. Each slide was stained with hypoxia-inducible factor 1a (HIF-1a) antibody and hypoxyprobe-1 anti-pimonidazole mouse monoclonal IgG1 antibody (MAb1). The percentage positivies for MAb1 and HIF-1a were quantified using ImageJ 1.41o software (National Institutes of Health) and compared between the two groups.

## **6. Statistical analysis**

All parameters were described as mean  $\pm$  standard deviation of mean for continuous variables. Statistical analyses were performed using a non-parametric Mann-Whitney U-test to evaluate the significance of differences in values between different areas. Pearson correlation test was performed to verify the relationships between density of immunohistochemistry stain and PET uptake. A P-value of  $<0.05$  was considered to indicate a statistically significant difference. All statistical procedures were performed using SPSS software (version 20.0; SPSS Inc., Chicago, IL, US).

### III. RESULTS

#### 1. Establishment of rat esophagectomy animal model

The vascular anatomy of rat stomach was similar to the vascular anatomy of human. Stomach was supplied from mainly left gastric, right gastric artery. The short gastric arteries and right gastroepiploic artery was poorly developed (Figure 2A). To establish the proper ischemia model, all blood vessels supplying stomach were ligated at first (complete devascularization, Figure 2B). After complete devascularization, blood supply was not detected on autoradiography (Figure 2C). Therefore partial devascularization saving the right gastroepiploic artery was done (Figure 2D), blood supply to stomach was maintained in autoradiography (Figure 2E). About 20 cases of rat esophagectomy were performed to establish the stable experiment.

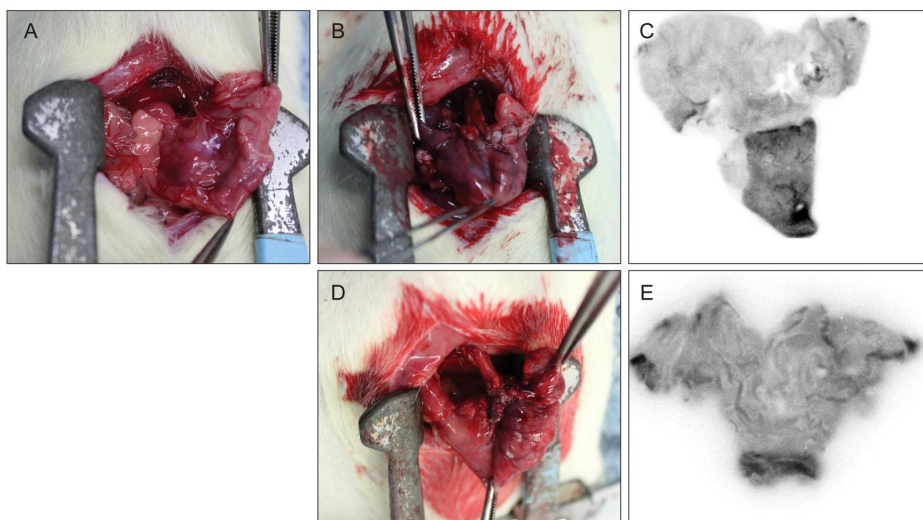
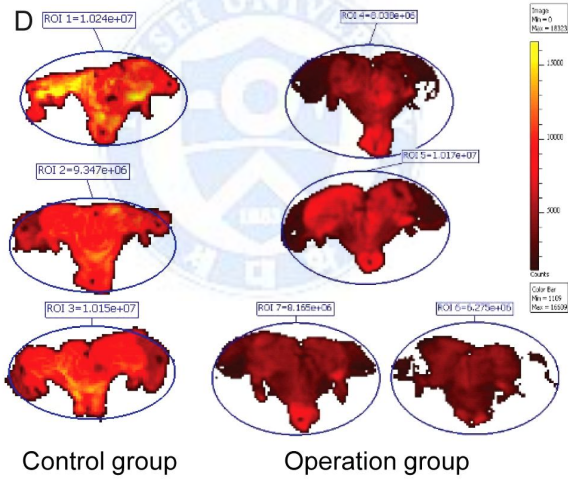
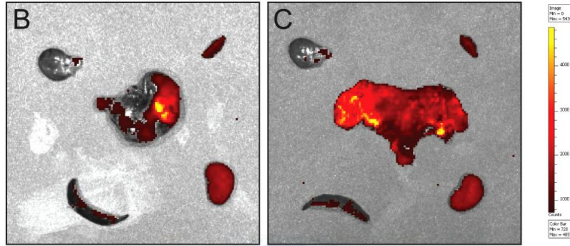
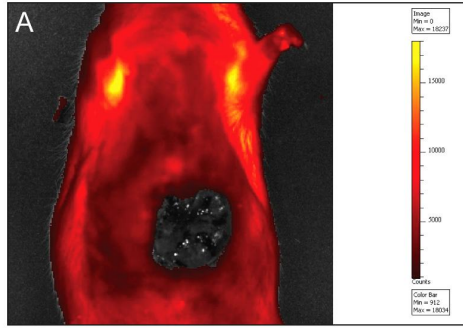


**Figure 2.** Rat esophagectomy animal model. A. Normal anatomy of rat stomach. B. Complete devascularization of stomach. C. Autoradiography after complete devascularization. D. Partial devascularization of stomach. E. Autoradiography after partial devascularization.

## **2. Fluorescent imaging**

As a pilot study, optical fluorescent imaging was taken in operation group. The optical imaging was taken in vivo status at first, but autofluorescence of hairs disturbs measuring the hypoxia status of in vivo stomach (Figure 3A). The rat was sacrificed and ex vivo optical fluorescent imaging was taken in operation group. The optical signals which meant hypoxia were increased at lesser curvature and fundus area of extracted whole stomach and it was obvious compared to other extracted organs such as heart, spleen, and liver. (Figure 3B and 3C)

Seven rats were each randomly assigned to the control (n=3) and the operation groups (n=4). Fluorescent imaging was taken in all together, for unifying the exposure time. The optical signals were compared between operation and control group in ex vivo status. The densities of optical imaging were not different between two groups. (Mann-Whitney test,  $p=0.2286$ , Figure 3C)



**E** Mann-Whitney test,  $p=0.2286$

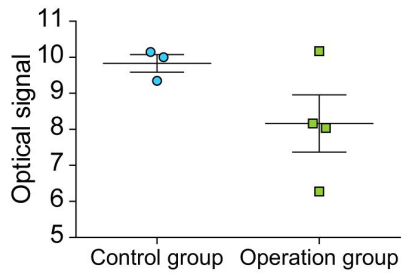


**Figure 3.** Fluorescent imaging. A. in vivo imaging in operation group. B. ex vivo imaging of stomach in operation group. C. ex vivo imaging of opened stomach in operation group. D. Optical ex vivo imaging in control group and operation group. E. Scatter dot plot for comparing the optical signals between control and operation group.

### 3. MicroPET imaging

Twelve rats were each randomly assigned to the control (n=6) and the operation groups (n=6). On static PET imaging, Cu-ATSM uptake at the fundus was observed in the operation group on the 3-h PET image (Figure 4A), but such abnormal  $^{64}\text{Cu}$ -ATSM uptake was not evident in the control group (Figure 4B). The mean %ID/g of the fundus in the operation group was  $0.047 \pm 0.015$ . In the control group, the area corresponding to the fundus was chosen as an ROI, because there was no definite area of uptake in the control group, and the mean %ID/g of this area was  $0.026 \pm 0.006$ ; the difference was significant (Mann-Whitney test,  $p=0.021$ , Figure 4C). The fundus/liver ratios were  $0.541 \pm 0.126$  and  $0.278 \pm 0.049$ , respectively (operation group and control group, Mann-Whitney test,  $p=0.002$ , Figure 4D).

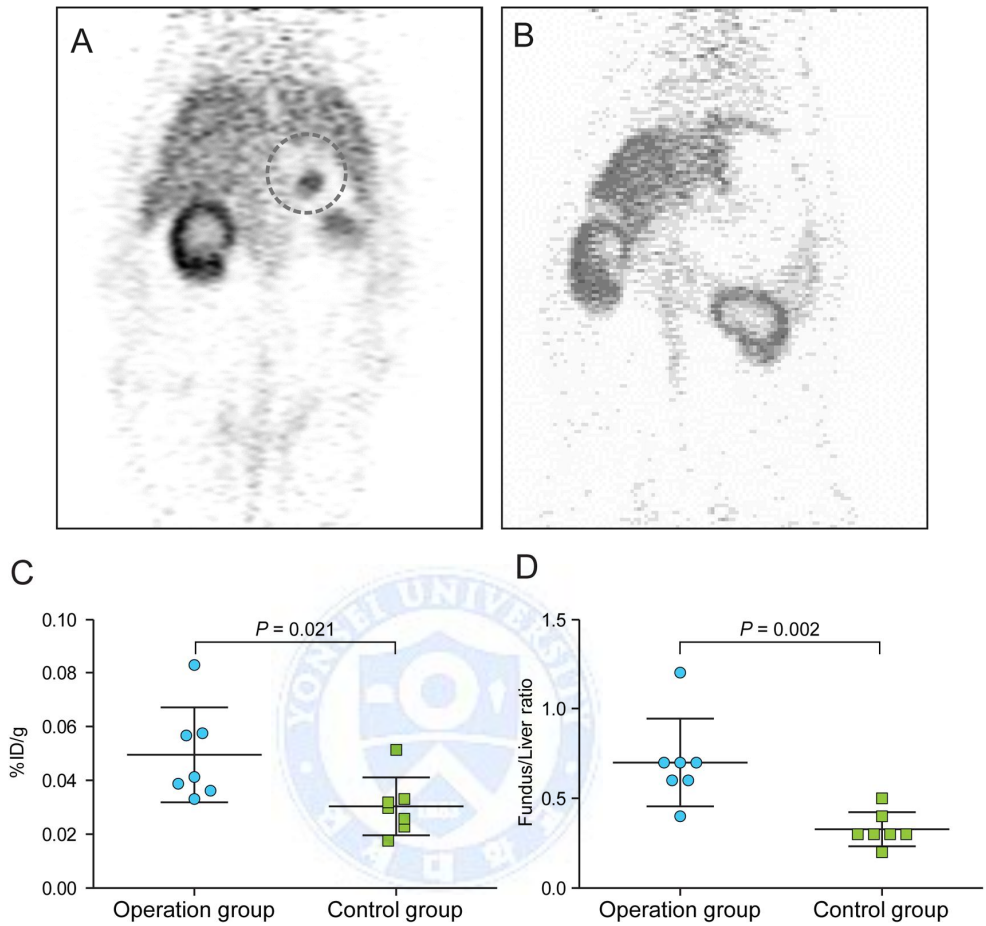


**Figure 4.** MicroPET imaging. A. Operation group. B. Control group. C. Scatter dot plot for comparing %ID/g values between the operation and control groups. D. Scatter dot plot for comparing the fundus/liver ratio (%ID/g of fundus area by %ID/g of liver) between the operation and control groups.

#### 4. Autoradiography

Autoradiographic images are shown in Figure 3. The principal region of  $^{64}\text{Cu}$ -ATSM uptake was the fundus in the operation group (Figure 5A). In the control group, no definite  $^{64}\text{Cu}$ -ATSM uptake by stomach tissue was evident (Figure 5B). The intensities of  $^{64}\text{Cu}$ -ATSM uptake are compared in Figure 5C;  $^{64}\text{Cu}$ -ATSM uptake was two-fold higher in the fundus than the greater curvature in the operation group ( $179.812 \pm 50.665$  PSL-BG vs.  $353.364 \pm 85.063$  PSL-BG, Mann-Whitney test,  $p < 0.001$ ), but, in the control group,  $^{64}\text{Cu}$ -ATSM uptake was similar in the fundus and greater curvature.

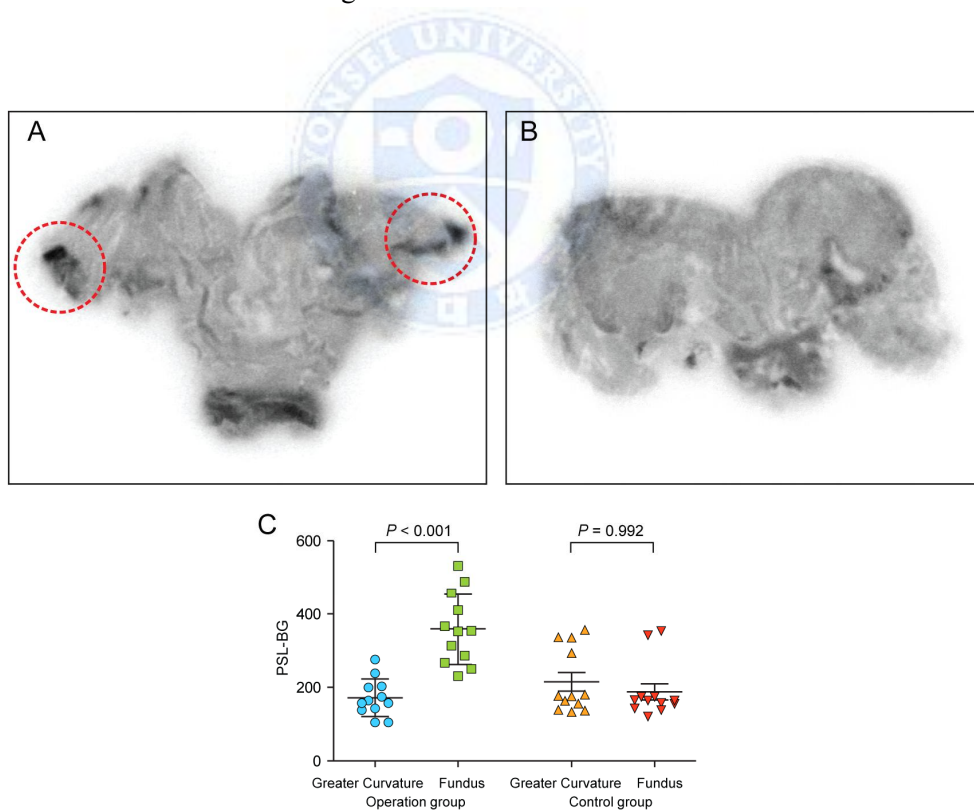


**Figure 5.** Autoradiography. A. Operation group. B. Control group. C. Scatter dot plot for comparing the intensities of  $^{64}\text{Cu}$ -ATSM uptake in the control and operation groups.

## 5. Immunohistochemistry

From the 12 rats, a total of 48 sections was prepared. The expression levels of pimonidazole and HIF-1a in the fundus and greater curvature were compared. In the operation group, pimonidazole and HIF-1a were expressed in the fundus but not the greater curvature (Figures 6A and 6B). In the control group, pimonidazole and HIF-1a expression was observed in neither the fundus nor the greater curvature (Figures 6C and 6D). In the operation group, pimonidazole and HIF-1a expression was significantly higher in the fundus than the greater curvature (Figures 6E and 6F).

The correlations between expression of immunohistochemistry and PET parameters were analysed. HIF-1a expression was correlated with both %ID/g and Fundus/Liver ratio (Pearson correlation 0.534,  $p < 0.001$  and Pearson correlation 0.593,  $p < 0.001$ , respectively. Figure. 7A and 7B). pimonidazole expression was also correlated with both %ID/g and Fundus/Liver ratio (Pearson correlation 0.386,  $p = 0.007$  and Pearson correlation 0.483,  $p = 0.001$ , respectively. Figure. 7C and 7D).

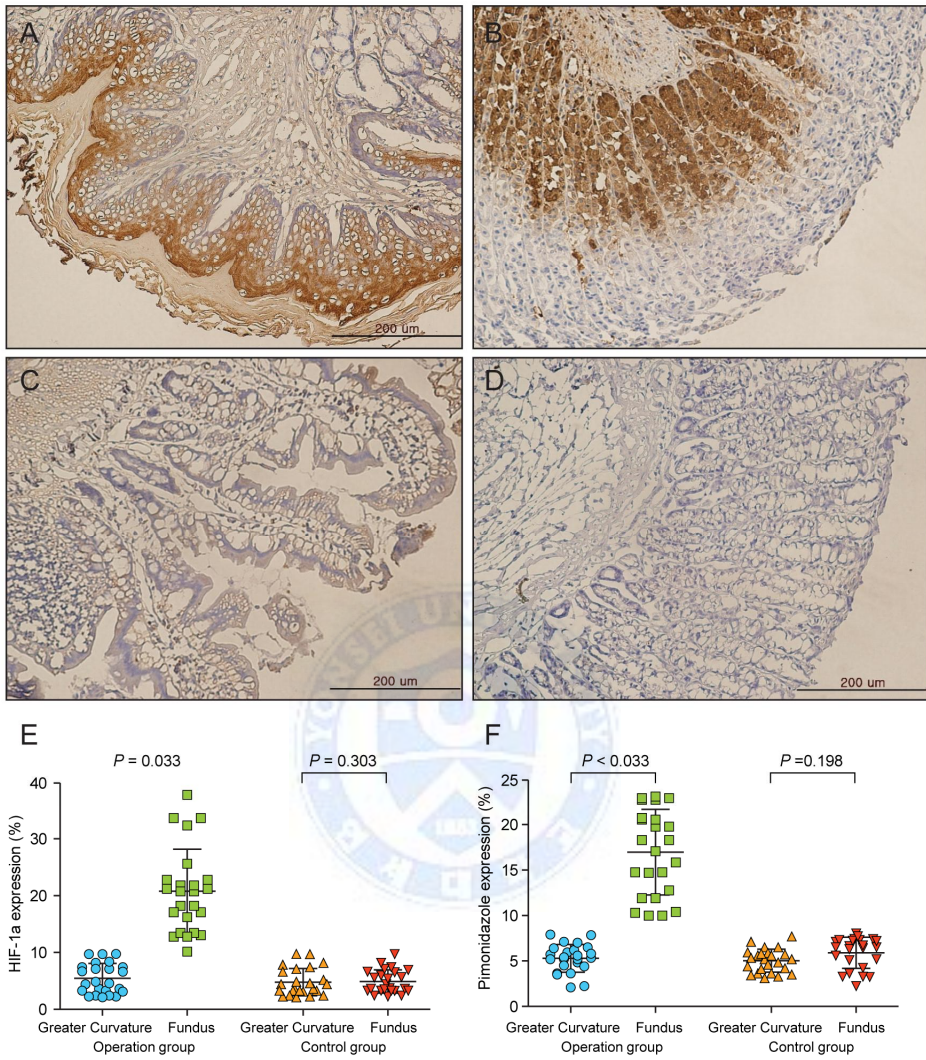


**Figure 6.** Immunohistochemistry. A. HIF-1a expression in the fundus of the operation group. B. Pimonidazole expression in the fundus of the control group. C. HIF-1a expression in the fundus of the control group. D. Pimonidazole expression in the fundus of the control group. E. Scatter dot plot comparing HIF-1a expression levels. F. Scatter dot plot comparing pimonidazole expression levels.

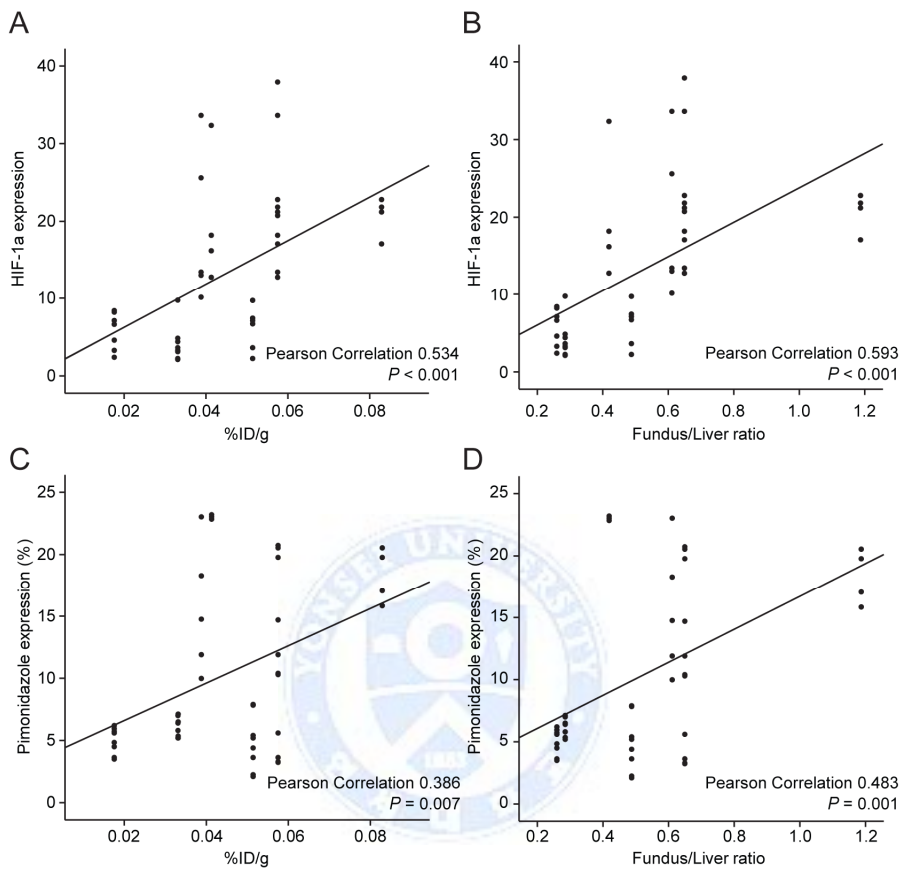


**Figure 7.** The correlations between expression of immunohistochemistry and PET parameters. A. HIF-1a expression and %ID/g. B. HIF-1a expression and Fundus/Liver ratio. C. Pimonidazole expression and %ID/g. D. Pimonidazole expression and Fundus/Liver ratio

#### **IV. DISCUSSION**

After esophagectomy and gastric reconstruction, anastomotic leakage develops in about 10% of patients. Ischemia of the gastric conduit is a major cause of this problem.<sup>2</sup> Mobilization of the stomach for gastric pull-up requires division of the left gastric, left gastroepiploic, and short gastric arteries. As the gastroepiploic arcade is rarely complete, the blood supply to the mobilized proximal stomach is largely derived from the rich submucosal plexus of vessels.<sup>7</sup> Although frank gangrene is rare if the stomach is properly mobilized,<sup>8</sup> occult ischemia of the gastric fundus often develops. Additionally, clinical detection and measurement of ischemia of the gastric conduit during the postoperative period is difficult. Chest CT is not useful and endoscopy is both subjective and invasive. Detecting and measuring ischemia of the gastric conduit in the postoperative period via a non-invasive imaging modality is essential to allow of decision-making in difficult clinical situations. After esophagectomy and gastric reconstruction, if ischemia of the gastric conduit is severe, take-down of the gastric conduit should be considered to avoid fulminant necrosis of the conduit and resulting sepsis. If ischemia is both mild and not extensive, conservative management can be considered.

In this study, we constructed rat esophagectomy model. Rat esophagectomy has been applied for studying the ischemic preconditioning, conduit perfusion and wound healing.<sup>5,6</sup> Opossum has most similar vascular anatomy of stomach compared to human's, but opossum is not available, we selected rat

esophagectomy model. In rat esophagectomy model, intrathoracic esophagectomy is not performed because it is fatal procedure to animal. Because rat has a long intraabdominal esophagus, intraabdominal esophagectomy and esophagogastronomy is performed instead of intrathoracic esophagectomy. Rat esophagectomy was relatively safe, feasible and reproducible animal model and it could be applied to other experiments.

First, we applied the optical fluorescent imaging for detecting the conduit ischemia. In general, substances that absorb light energy change to an unstable excitation state from the ground state and then revert back to the ground state after energy transition. This energy transition includes vibrational energy, heat energy, and light energy (fluorescence). In some pathologic conditions, body emits the fluorescence, autofluorescence imaging is most commonly used for ocular and gastrointestinal imaging, and is useful for detecting early esophageal squamous cell carcinoma<sup>9,10</sup>. In exogenous fluorophores which injected into lymphatics has been applied in detecting the sentinel lymph nodes in breast cancer. In this study, we used Hypoxia fluorescent probe Hypoxisense 680 which is quenched by oxygen and is increased in response to low levels of oxygen was used. Hypoxisense 680 permeates cell membrane and it is possible to determine cellular hypoxia by red-fluorescence imaging. In pilot study, high uptake of Hypoxisense 680 was observed in operation group. However, in comparison with control group, the uptake of Hypoxisense 680 was not significantly different. This study showed that optical fluorescent imaging with exogenous hypoxia fluorescent is not appropriate for detecting the conduit

ischemia. Actually, there are several limitations of fluorescent imaging for detecting the conduit ischemia. First, infra-red rays in fluorescent imaging have shallow penetration depths. It could not penetrate even skin layers, therefore we obtained imaging under laparotomy status. In clinical situation, it could be applied with endoscopy because of shallow penetration. Second, hairs and food materials make the autofluorescence and it can be an artifact of image. These limitations might be related to negative results of optical fluorescent imaging in this study.

We hypothesized that hypoxia PET imaging would detect conduit ischemia. In fact, ischemia and hypoxia are different phenomena: ischemia refers to low blood circulation in a particular tissue or cell, whereas hypoxia refers to low-level oxygen saturation in a particular tissue or cell. Nevertheless, hypoxia was generally present in ischemic areas in several previous studies. Some researchers have reported that HIF-1a is expressed in ileal mucosa cells after superior mesenteric artery occlusion or hemorrhagic shock (ischemia) in rats.<sup>11</sup> Clinically, hypoxia imaging has been applied to study acute cerebral ischemia, using hypoxia-detecting agents such as 18F-fluoromisonidazole.<sup>12</sup> Although ischemia and hypoxia differ, they seem to share a common pathophysiology. Based on these observations, we attempted to use hypoxia PET imaging to detect ischemia of a gastric conduit, using the rat esophagectomy model described on previous studies.<sup>5,6</sup> As esophagectomy and reconstruction are very invasive and associated with high mortality, intrathoracic esophagectomy with

anastomosis is difficult to perform in animals. Fortunately, the intraabdominal esophagus of the rat is relatively long, and previous investigators successfully performed partial resection of this section of the esophagus, and intraabdominal anastomosis, in the rat.<sup>5,6</sup> Also, the vascular anatomy of the rat stomach is quite similar to that of the human. This animal model seeks to mimic gastric ischemia, not intrathoracic esophagectomy and/or gastric pull-up. We performed 20 rat esophagectomies prior to initiation of main experiment.

We used  $^{64}\text{Cu}$ -ATSM as a radiotracer for hypoxia imaging in this study with two reasons. First,  $^{64}\text{Cu}$ -ATSM is very lipophilic with low molecular weight, therefore is more permeable to high cell membrane than other imidazole-ring group hypoxia agents such as  $^{18}\text{F}$ -fluoromisonidazole (fMISO).  $^{64}\text{Cu}$ -ATSM can permeate the cell membrane freely and converted from  $^{64}\text{Cu}^{2+}$ -ATSM to  $^{64}\text{Cu}^{1+}$ -ATSM in cell.  $^{64}\text{Cu}^{1+}$ -ATSM cannot permeate the cell membrane and deposit in the cell. To convert from  $^{64}\text{Cu}^{1+}$ -ATSM to  $^{64}\text{Cu}^{2+}$ -ATSM needs normoxia status.<sup>13,14</sup> Second, Cu-ATSM has been studied not only in tumor conditions but also in non-tumor conditions such as myocardial perfusion and cerebral ischemia, in contrast to other imidazole-ring group hypoxia tracers which has been studied mainly in tumor conditions.<sup>15-17</sup> On  $^{64}\text{Cu}$ -ATSM PET imaging, radiotracer uptake was observed in the fundus of the operation group. The gastric fundus is the area most susceptible to ischemia after ligation of the left gastric and short gastric arteries. The area of  $^{64}\text{Cu}$ -ATSM uptake on PET

imaging was correlated with the results of autoradiography. In the operation group, HIF-1a and pimonidazole expression was also noticed in the fundus, whereas HIF-1a and pimonidazole were not expressed in the greater curvature. These results suggest that  $^{64}\text{Cu}$ -ATSM PET imaging can detect ischemia of the gastric conduit after devascularization. Hypoxia imaging has been used in several fields, mainly oncology and imaging of stroke patients. In oncology, the ability to determine the degree and extent of tumor hypoxia is important both prognostically and to select patients requiring hypoxia-directed therapies. Also, hypoxia PET imaging can be used in stroke victims to distinguish severely hypoxic viable tissue from reperfused or necrotic tissue<sup>18</sup>. Our study suggests a new potential application of hypoxia imaging after esophagectomy to detect conduit ischemia, which could be very useful in the perioperative management of patients undergoing esophagectomy.

This study had some limitations. First, we could not study whether conduit ischemia was associated with clinical outcomes such as anastomotic leakage. However, to obtain the image of autoradiography and immunohistochemistry, the rats had to be euthanized on postoperative day 1. In addition, we thought that the ischemia was most severe at postoperative day 1 and resolved as blood perfusion gradually recovered. In this experiment, we tested whether hypoxia PET imaging was able to detect ischemia per se as a preliminary experiment. Whether conduit ischemia was associated with anastomotic leakage should be

explored in further animal studies with longer follow-up periods. Second, more clinical work is needed to verify whether our findings would be useful in human medicine. Finally, several studies reported that Cu-ATSM has tumor type-specific hypoxia selectivity with raising a question as universal hypoxia tracer,<sup>19,20</sup> and they suggested that the avid binding of Cu-ATSM to specific tumors might involve other mechanisms independent of hypoxia. However, <sup>64</sup>Cu-ATSM has been accepted as a safe radiopharmaceutical that can be used to obtain high-quality images of tumor hypoxia in human cancers and other non-tumor conditions.<sup>15-17,21</sup>



## V. CONCLUSION

This study showed that  $^{64}\text{Cu}$ -ATSM hypoxia PET imaging could detect ischemia of a gastric conduit after devascularization in a rat esophagectomy model. Further animal and clinical studies are needed to verify whether hypoxia imaging could be used toward this end in humans.



## REFERENCES

1. Müller J, Erasmi H, Stelzner M, Zieren U, Pichlmaier H. Surgical therapy of oesophageal carcinoma. *British Journal of Surgery* 1990;77:845-57.
2. Urschel JD. Esophagogastronomy anastomotic leaks complicating esophagectomy: a review. *The American journal of surgery* 1995;169:634-40.
3. Valverde A, Hay J-M, Fingerhut A, Elhadad A. Manual versus mechanical esophagogastric anastomosis after resection for carcinoma: a controlled trial. *Surgery* 1996;120:476-83.
4. Oezcelik A, Banki F, Ayazi S, Abate E, Zehetner J, Sohn HJ, et al. Detection of gastric conduit ischemia or anastomotic breakdown after cervical esophagogastronomy: the use of computed tomography scan versus early endoscopy. *Surgical endoscopy* 2010;24:1948-51.
5. Cui Y, Urschel JD, Petrelli NJ. Esophagogastric Anastomoses in Rats- An Experimental Model. *Investigative Surgery* 1999;12:295-8.
6. Urschel JD, Antkowiak JG, Delacure MD, Takita H. Ischemic conditioning (delay phenomenon) improves esophagogastric anastomotic wound healing in the rat. *Journal of Surgical Oncology* 1997;66:254-6.
7. Thomas D, Langford R, Russell R, Le Quesne L. The anatomical basis for gastric mobilization in total oesophagectomy. *British Journal of Surgery* 1979;66:230-3.

8. Moorehead R, Wong J. Gangrene in esophageal substitutes after resection and bypass procedures for carcinoma of the esophagus. *Hepato-gastroenterology* 1990;37:364-7.
9. Yoshida Y, Goda K, Tajiri H, Urashima M, Yoshimura N, Kato T. Assessment of novel endoscopic techniques for visualizing superficial esophageal squamous cell carcinoma: autofluorescence and narrow-band imaging. *Diseases of the Esophagus* 2009;22:439-46.
10. Suzuki H, Saito Y, Ikehara H, Oda I. Evaluation of visualization of squamous cell carcinoma of esophagus and pharynx using an autofluorescence imaging videoendoscope system. *Journal of gastroenterology and hepatology* 2009;24:1834-9.
11. Koury J, Deitch EA, Homma H, Abungu B, Gangurde P, Condon MR, et al. Persistent HIF-1 $\alpha$  activation in gut ischemia/reperfusion injury: potential role of bacteria and lipopolysaccharide. *Shock* 2004;22:270-7.
12. Read S, Hirano T, Abbott D, Sachinidis J, Tochon-Danguy H, Chan J, et al. Identifying hypoxic tissue after acute ischemic stroke using PET and 18F-fluoromisonidazole. *Neurology* 1998;51:1617-21.
13. Imam SK. Review of positron emission tomography tracers for imaging of tumor hypoxia. *Cancer biotherapy & radiopharmaceuticals* 2010;25:365-74.
14. Takahashi N, Fujibayashi Y, Yonekura Y, Welch MJ, Waki A, Tsuchida T, et al. Evaluation of <sup>62</sup>Cu labeled diacetyl-bis (N 4-methylthiosemicarbazone) as a hypoxic tissue tracer in patients with lung cancer. *Annals of nuclear medicine* 2000;14:323-8.

15. Fujibayashi Y, Cutler C, Anderson C, McCarthy D, Jones L, Sharp T, et al. Comparative studies of Cu-64-ATSM and C-11-acetate in an acute myocardial infarction model: ex vivo imaging of hypoxia in rats. *Nuclear medicine and biology* 1999;26:117-21.
16. Isozaki M, Kiyono Y, Arai Y, Kudo T, Mori T, Maruyama R, et al. Feasibility of <sup>62</sup>Cu-ATSM PET for evaluation of brain ischaemia and misery perfusion in patients with cerebrovascular disease. *European journal of nuclear medicine and molecular imaging* 2011;38:1075-82.
17. Takahashi N, Fujibayashi Y, Yonekura Y, Welch MJ, Waki A, Tsuchida T, et al. Copper-62 ATSM as a hypoxic tissue tracer in myocardial ischemia. *Annals of nuclear medicine* 2001;15:293-6.
18. Takasawa M, Moustafa RR, Baron J-C. Applications of nitroimidazole in vivo hypoxia imaging in ischemic stroke. *Stroke* 2008;39:1629-37.
19. Yuan S, Yu Y, Chao KC, Fu Z, Yin Y, Liu T, et al. Additional value of PET/CT over PET in assessment of locoregional lymph nodes in thoracic esophageal squamous cell cancer. *Journal of Nuclear Medicine* 2006;47:1255-9.
20. Matsumoto I, Oda M, Takizawa M, Waseda R, Nakajima K, Kawano M, et al. Usefulness of fluorine-18 fluorodeoxyglucose-positron emission tomography in management strategy for thymic epithelial tumors. *The Annals of thoracic surgery* 2013;95:305-10.
21. Lewis JS, Laforest R, Dehdashti F, Grigsby PW, Welch MJ, Siegel BA. An imaging comparison of <sup>64</sup>Cu-ATSM and <sup>60</sup>Cu-ATSM in cancer of the uterine cervix. *Journal of Nuclear Medicine* 2008;49:1177-82.

## ABSTRACT (IN KOREAN)

Hypoxia imaging을 통한 랫트 식도절제술 모델에서 위장관  
튜브의 허혈 여부 진단법 개발

<지도교수 정 경 영>

연세대학교 대학원 의학과

박 성 용

위장관튜브의 허혈은 식도 절제술 및 식도위문합술 이후 발생하는 문  
합부위누출과 문합부위 협착의 주된 원인으로 알려져 있다. 이러한  
위장관튜브의 허혈을 찾아내는 것은 임상적으로 매우 중요하나 현재  
의 영상학적 방법으로는 허혈을 찾는 것이 어렵다. 본 연구에서는 형  
광영상과 PET 영상을 통하여, 이러한 영상기법들이 랫트 식도 절제  
술 모델에서 위장관튜브의 허혈을 찾아낼 수 있는지 여부를 확인하고  
자 하였다. 랫트 식도 절제술 모델은 12-16주 된 300-350 g 의  
Sprague-Dawley 랫트를 사용하였다. 실험군에서는 left gastric  
artery와 short gastric artery를 결찰하고 식도위연결부위를 일부 절  
제하고 문합하였다. 대조군에서는 혈관 결찰을 하지 않은 상태에서  
식도위연결부위를 절제 후 문합하였다. 수술 후 24시간 후에 형광 영

상과  $^{64}\text{Cu}$ -diacetyl-bis (N4-methylsemicarbazone) ( $^{64}\text{Cu}$ -ATSM) 을 사용한 PET 영상을 시행하였다. 동물실험에서 형광 영상은 위장관 튜브의 허혈을 확인하기 어려웠다. 그러나  $^{64}\text{Cu}$ -ATSM을 사용한 PET 영상에서는 위장관 튜브의 기저부에서 허혈 부위를 확인 할 수 있었다. 수술군의 기저부에서의 %ID/g은 대조군의 기저부보다 통계적으로 유의하게 높았으며 ( $0.047 \pm 0.015$  vs.  $0.026 \pm 0.006$ ,  $p=0.021$ ), 간/기저부 비율또한 수술군에서 유의하게 높았다. ( $0.541 \pm 0.126$  vs.  $0.278 \pm 0.049$ ,  $p=0.002$ ). 자가조직방사선촬영술 (autoradiography) 상에서,  $^{64}\text{Cu}$ -ATSM 의 섭취가 수술군의 위장관 튜브 기저부에서 발견되었으며, 이 결과는 PET 영상과 일치하였다. 면역형광영상에서 hypoxia-inducible factor 1a 와 pimonidazole 의 염색이 위장관 튜브의 기저부위에서 명확하게 나타났다. 본 연구 결과  $^{64}\text{Cu}$ -ATSM을 사용한 PET 영상은 랫트 식도절제술 모델에서 위장관 튜브의 허혈을 확인 할 수 있었으며, 이 결과가 임상에 적용될 수 있는지는 추가적인 연구를 통해 검증해야 할 것이다.

---

핵심되는 말: 식도절제술, 위장관 튜브 허혈, hypoxia imaging, PET